TENTH AUSTRALASIAN FLUID MECHANICS
CONFERENCE - UNIVERSITY OF MELBOURNE
11-15 DECEMBER 1989

Keynote Paper KS-10

DEVELOPMENTS IN DETONATION THEORY

J.F. CLARKE

College of Aeronautics
Cranfield Institute of Technology
Bedford
ENGLAND

ABSTRACT

Examples are given of two distinct ways in which thermal runaway, coupled with propagation of compression or shock waves, can be established in combustible gas mixtures. Various features such as unsteady induction domains, quasi-steady combustion waves and reaction-induced shocks are identified, using a mixture of asymptotic analysis and numerical computational methods, all with a view to understanding the processes through which detonation waves evolve. It is demonstrated that the unsteady induction domain, in which disturbance amplitudes are small, exerts a powerful influence on the way the fields develop.

1. MOTION PRODUCED BY HEAT POWER

Suppose that energy is transmitted by heat conduction through the fixed impermeable surface $x = 0$ into a plane half-space of cold combustible gas in $x > 0$. After a brief interval of time, $0 < t < t_d$ (cf Fig.2), during which heat-conduction is the dominant process within a thermal boundary-layer adjacent to $x = 0$, a plane shock wave emerges from this conduction-dominated layer and propagates out into $x > 0$ as the precursor to some more-or-less intense combustion activity. The heat-power-input is chosen so as to give rise to a precursor shock that lowers induction (or, loosely, ignition) times by factors of the order of 10^{-5}; gas ahead of the shock is thereby chemically inert for all practical purposes. Fig. 1 exhibits instantaneous temperature T and pressure p profiles which have been computed as numerical solutions of the Navier-Stokes equations for the situation described above (Clarke, et al, 1986, 1989), with combustion taking place via a simple irreversible first-order Arrhenius reaction. The profiles are illustrative of the situation over a range of times prior to an "explosion" time t_e, as shown in Fig.2. Apart from the precursor shock PS, Figs.1 and 2 identify an induction domain I, a combustion wave CW (within which there is significant increase of temperature and associated decrease of pressure), and a plateau of substantially uniform conditions followed by the thermal boundary-layer TBL adjacent to $x = 0$.

Fig.3, which is lettered to correspond with Fig.1, is a picture of p versus v, the specific volume, through the whole field whose profiles are depicted in Fig.1. The points O and S_a, which represent the ambient, cold, atmosphere and the immediate post-precursor-shock condition, respectively, lie on the unreacted Hugoniot curve $\mathcal{H}_0(1)$ whose "origin" is O. It can be seen that the hot, relatively low-pressure, parts of CW adjacent to point E lie on a straight line $\mathcal{L}_F$, which intersects $\mathcal{H}_0(1)$ at point S. The computations confirm that all of the reactant material is consumed by the time point E is reached and, consistent with this, it can also be seen that point E in Fig.3 lies on the "all-reacted" Hugoniot curve whose "origin" is S, namely $\mathcal{H}_s(0)$.

Since Fig.1 illustrates a solution of the Navier-Stokes equations it is to be anticipated that precursor shock OS_a has a continuous structure and this is evident from the figure. The fact that the shock is rather thick in relation to the spatial extent of both I and CW, which are regions of primary influence of the chemical reaction, is indicative of the fact that general diffusive effects for mass, momentum and energy have been exaggerated. It is well known that the existence of several disparate time scales creates a problem in the numerical modelling of situations for which they occur (Oran and Boris, 1981), and it is to alleviate such problems that Clarke, et al, (1986), (1989) chose to magnify the diffusive time scale. However, despite this, the results obtained by these authors show that, away from the interiors of shock OS_a and boundary-layer TBL, even the magnified diffusive effects are small enough to be neglected. The field from S_a, through F, and on past E towards the wall at $x = 0$ is therefore effectively diffusionless or inviscid, and behaviour in these regions can be discussed in terms of the Euler rather than the Navier-Stokes equations.

In the circumstances that have just been described, it is clear that $\mathcal{L}_F$ in Fig.3 is a Rayleigh line. As such, it follows that the (large) part of CW adjacent to point E is behaving, instantaneously, like a diffusionless combustion wave. One is entitled to use the word wave here because of the clear implication from Fig.2 that CW propagates in the direction of x-increasing, doing so in fact with Mach numbers in the region of 0.27 to 0.29 (in the examples computed so far) at point S of Fig.3. The implication is that CW here is a deflagration or fast flame through which pressure falls steadily in the direction of the flow.

Prior to time t_e, CW has all the attributes of a quasi-steady wave. Changes do take place, albeit very slowly prior to time t_e, in both PS, which strengthens, and CW, which also strengthens in the sense that the speed of outflow from the left-hand side of the wave (relative to the quasi-steady wave itself) begins to approach the local speed of sound (Clarke, et al, 1989). In the

terms of Fig.3, the latter is equivalent to a slow change in the relationship between $\mathcal{L}_F$ and $\mathcal{H}_s(0)$ towards a condition of tangency at E; in other words, towards the Chapman-Jouguet condition.

Although such slow changes are important it is more important to observe that the domain I is essentially unsteady. Furthermore it is a region within which chemical changes, although small in amplitude, are nonetheless significant, as will be explained in §3.

After time t_e the picture changes significantly and quite swiftly. Combustion wave CW momentarily loses its identify, reaction spreads over a wider region of space RC (for "reaction centre"; cf Fig.2), density (which has been falling from PS through I and into CW prior to t_e) begins to increase within RC, which rapidly takes the form of a localised compression pulse. A new combustion wave CW then emerges, travelling much more quickly, and a shock, RS, forms at its head. The whole combination of reaction-induced shock RS and CW makes a rapid transition to become a Zeldovich-von Neumann-Doring (ZND) detonation wave.

2. MOTION PRODUCED BY MECHANICAL POWER

Now suppose that the same combustible gas mixture as the one described in §1 is set in motion by the purely mechanical method of pushing it into $x > 0$ by means of a piston.

This situation has been evaluated by using the numerical random choice method (RCM) to solve the Euler equations, as described by Clarke and Singh (1989). Fig.4 illustrates some of the important features that emerge from these calculations; P is the piston, set in motion at time = 0, which drives precursor shock PS into cold unreacted gas. As in the situation described in §1, PS lowers induction times by a large factor and so switches on significant chemical activity in an induction domain I. At first the maximum rate of chemical reaction occurs on the piston face, but at some time t_e, near to point D, reaction becomes exceptionally rapid and a reaction centre RC is formed. The maximum-reaction-rate path detaches itself from RC and follows the path labelled CW in Fig.4. Fig.5 is a picture of chemical reaction rate versus time for a number of fluid particles as they traverse CW. One such particle path, labelled ψ, is shown in Fig.4 and it is pertinent to remark that the calculations were made using Lagrangian ψ,t variables.

There is evidence (cf §§3,4 below) that CW starts to travel away from D at very high speeds. Pressure and density levels increase rapidly within CW, as can be seen in Figs. 6 and 7, which show p and ρ versus time for several fixed-ψ particle paths. Fig.8 shows p-v loci for several ψ-values, with particle travel marked from (a) to (b) to (c), through CW, both in Fig.8 and in Fig.4. For the largest ψ-value illustrated in Figs.6, 7 and 8 there is unequivocal evidence (provided by RCM) for the existence of a shock-wave RS that has been born from activity within the combustion wave CW. For values of ψ that are slightly larger than the ones depicted in Figs.6 - 8 it is found that the combination of RS and CW has made the final transition to a ZND detonation.

There are clearly differences as well as similarities between the situations illustrated in Figs. 2 and 4. Similarities have been emphasised by using the same labelling in each figure where this is appropriate.

Differences are not quite so evident from Figs.2 and 4 alone. One large difference lies in the speed of propagation of CW in the two cases. For times $t < t_e$ in Fig.2, CW propagates into I at subsonic speeds, whilst CW in Fig.4 propagates into I at supersonic speeds. Thus, whilst it is proper to call each propagating region of intense chemical activity a combustion wave, it is evident that their detailed character, or structure, will be different in the two situations. A fluid particle crosses CW in Fig.2, which is a quasi-steady fast flame for $t < t_e$, from (a) to (b), as indicated on the line labelled ψ in that figure. Pressure falls from (a) to (b). The situation is rather less clear-cut in Fig.4 where a particle traverses CW from (a), through (b) near the location of maximum reaction rate and then emerges at (c). Pressure rises from (a) to (b) and falls from (b) to (c), with the rise taking place, at least in its early stages from (a), roughly along a Rayleigh line $\mathcal{L}$ (Fig.8). There is reason (cf §4 below) to believe that (a) $\rightarrow$ (b) is a transition through a quasi-steady weak detonation, and that (b) $\rightarrow$ (c) is then an expansion wave that follows the weak-detonation in order to reconcile the motion with the velocity boundary condition P. If this construction is exactly true, chemical reaction should cease at (b) and (b) should lie on an appropriate "all-reacted" Hugoniot curve. Reaction does not cease at (b) and it appears that weak-detonation and expansion are merged in this neighbourhood. This is probably due to an insufficiently sharp dependence of reaction rate on local temperature (cf §3) in the calculations by Clarke and Singh (1989).

It is interesting to remark on the similarity that exists between the two situations in Figs.2 and 4 for times $t > t_e$ during which the detonation wave is born.

Two particular features emerge from the discussion so far. One is the existence of propagating combustion waves in a situation for which diffusion, in its broadest sense, is effectively absent and the other is the existence of a class of unsteady induction domains within which chemical reaction and flow dynamics have equal status. Each one is discussed in more detail in the sections that follow, making use of asymptotic analysis.

3. INDUCTION DOMAIN

Any fluid particle that crosses precursor shock PS enters induction domain I. Assume that behaviour downstream of PS is adequately described by the Euler equations; using Lagrangian co-ordinates these can be written down in the form

$$v_t = u_\psi \ , \ \gamma u_t = -p_\psi \ , \qquad 3.1,2$$

$$\gamma p v_t + v p_t + \gamma Q c_t = 0 \ , \qquad 3.3$$

$$c_t + \Phi = 0 \ . \qquad 3.4$$

The variables are all dimensionless, as follows: p, v and c are pressure, specific volume and reactant mass fraction, respectively, measured in units of p_i', v_i' and c_i' where subscript-i denotes a constant reference state and a prime ()' implies a dimensional or un-normalised quantity; u is gas velocity measured in units of sound speed $a_i' = (\gamma p_i' v_i')^{\frac{1}{2}}$, where γ is a constant ratio of specific heats; t is time measured in units of an induction time t_{Ii}' and ψ is the Lagrange co-

ordinate in units of $a_i' t_{Ii}'/v_i'$; $Q = (\gamma-1)Q' c_i'/p_i' v_i'$ where Q' is heat of reaction per unit mass of reactant; finally Φ is the chemical reaction rate (strictly, a frequency or reciprocal of a time) divided by c_i'/t_{Ii}'.

It is perfectly adequate for present purposes to model the chemical reaction as one of first order that proceeds via Arrhenius kinetics with activation energy E_A'. In the circumstances a physically acceptable model for Φ is

$$Q\Phi = \varepsilon \exp\{(T-1)/\varepsilon T\} c \ , \qquad 3.5$$

It will be assumed that $\varepsilon \ll 1$, since it is a measure of the sensitivity of chemical reaction rate to changes of temperature. Asymptotic analysis of (3.1-5) is carried out in the limit as $\varepsilon \to 0$.

Assume that conditions $()_i$ are those which prevail immediately downstream of shock PS at a particular time, such as t_d (Fig.2) or zero (Fig.4), at which PS, I and CW have become distinct domains, away from the influences of diffusion. Subsequent events in I at least, can be followed for some time after t_d by looking for asymptotic approximate solutions of (3.1-5) in the form

$$f(\psi,t;\varepsilon) \sim f_i + \varepsilon \tilde{f}(\psi,t) \ ; \ f = p,v,c,u, \qquad 3.6$$

in the limit as $\varepsilon \to 0$ with ψ,t fixed. The (constant) quantities f_i are equal to 1 when f is p, v or c and equal to the Mach number of the flow immediately behind PS (which is O(1) as $\varepsilon \to 0$) at time t_d in Fig.2 or time zero in Fig.4.

Perturbation quantities $\tilde{f}$, and their derivatives with respect to ψ and t, are O(1) in the ε-limit, by hypothesis. The implication is that time and length scales for significant variations in I are indeed t_{Ii} and $a_i t_{Ii}$; as a consequence it can be stated that time-variations of f (cf(3.6)) are $O(\varepsilon)$ on <u>any</u> path in I that travels with speed less than or equal to the local sound speed, which is 1 to leading order in I.

In the circumstances (3.1-5) reduces to the following system of equations:

$$\tilde{v}_t - \tilde{u}_\psi = 0 \ , \quad \gamma \tilde{u}_t + \tilde{p}_\psi = 0 \qquad 3.7,8$$

$$\gamma \tilde{v}_t - \tilde{p}_t = \gamma \exp \tilde{T} \ ; \ Q\tilde{c}_t = -\exp \tilde{T} \ , \qquad 3.9;10$$

and $\tilde{T} = \tilde{p} + \tilde{v}$ is the temperature perturbation. These equations can be written in various ways to illustrate various features of the I-domain. First,

$$\tilde{p}_t \pm \tilde{p}_\psi \pm \gamma(\tilde{u}_t \pm \tilde{u}_\psi) = \gamma \exp \tilde{T} \qquad 3.11$$

(taking either upper or lower signs together) shows that propagation of $\tilde{p}$ and $\tilde{u}$ disturbances along (acoustic) wavelets $d\psi/dt = \pm 1$ is influenced by the combustion reaction acting as a source term ($\gamma \exp \tilde{T}$). Second,

$$(\gamma-1)\tilde{p}_t = \gamma\{\tilde{T}_t - \exp\tilde{T}\}, (\gamma-1)\tilde{v}_t = -\{\tilde{T}_t - \gamma \exp \tilde{T}\}, \qquad 3.12,13$$

show how $\tilde{T}$ would change with time if either pressure or specific volume was constant. Third, noting that (3.7 and 8) together make $\gamma \tilde{v}_{tt} + \tilde{p}_{\psi\psi} = 0$, it quickly follows that $\tilde{T}$ satisfies the third-order partial differential equation

$$\{\tilde{T}_t - \gamma \exp \tilde{T}\}_{tt} - \{\tilde{T}_t - \exp \tilde{T}\}_{\psi\psi} = 0. \qquad 3.14$$

Evidently the induction domain is a region within which competing tendencies to thermal runaway at either constant volume or constant pressure are resolved by the presence of acoustical waves that travel at speeds between ± 1 (cf the operator $\tilde{T}_{ttt} - \tilde{T}_{t\psi\psi}$) and $\pm \gamma^{-1/2}$ (cf operator $\gamma(\exp\tilde{T})_{tt} - (\exp \tilde{T})_{\psi\psi}$).

Equation (3.14) has some interesting properties (Clarke, 1981, 1985), but dominant amongst them is the fact $\tilde{T} \to \infty$ like $-\ln\{\gamma(t_e - t)\}$ as t approaches an explosion time t_e at some point or location within the field generated by a variety of boundary- and/or initial-value data (Clarke and Cant(1984); Jackson and Kapila (1985) for "piston problems": Cant (1984) for "contact-surface" driven flows: Dold (1988); Jackson, Kapila and Stewart (1987) for initial $\tilde{T}$-values with a single maximum). Furthermore $\tilde{p} \to \infty$ like $-\ln\{A(t_e - t)\}$ where A is a O(1) constant. Density variations in the vicinity of thermal runaway (equal to $1-\varepsilon v$ to $O(\varepsilon)$) remain bounded, since $\tilde{v} \to \ln(A/\gamma)$. Note that the value of A will depend upon the particular conditions that precede, and indeed control, the runaway process.

Solutions of (3.7-9) have all been obtained numerically, with one interesting exception. Blythe and Crighton (1989) have exploited the asymptotic limit $(\gamma-1) \to 0$ to study the situation in Fig.4 prior to t_e. Their results agree remarkably well with the numerical studies (cf authors quoted in the previous paragraph), which have all been made for $\gamma = 1.4$.

When $t_e - t \equiv \tau \to 0$ it is valuable to examine the structure of the thermal runaway region by analytical means. There are obviously a number of different physical situations in which runaway or reaction-centre behaviour will be encountered (indeed Figs. 2 and 4 illustrate two of them) and there is still much to do before understanding is complete. Two particular situations have been studied so far; both involve initial-value problems for (3.7-9). Jackson, et al, (1987) have dealt with the case of a single, symmetrical, $O(\varepsilon)$ -peak distribution in T-1, and with the situation in $x > 0$ for which $T_x(0,0) < 0$ (this is in essence what happens in Fig.4 for $t \to t_e$). Dold (1988) has also analysed the symmetrical case.

Physical arguments show that in either of these two situations runaway, or the generation of a reaction centre RC (cf Figs. 2,4), takes place at a particular point in ψ,t space, which suggests that independent variables that "focus" on such a point will be useful. For the problem illustrated in Fig.4 it is clear that runaway first occurs near $D(\psi = 0, t = t_e)$; variables of the form

$$\tau \equiv t_e - t \ , \ \psi/\sigma(\tau) \ , \qquad 3.15$$

where $\sigma(\tau \to 0) \to 0$, are required. Jackson, et al, find a central core to the runaway domain in which $\sigma(\tau) = \tau$ and, outside of this, a larger region for which

$$\sigma(\tau) = \tau^n, \ \tfrac{1}{2} < n < 1 \ . \qquad 3.16$$

The index n is equal to $\gamma/(2\gamma-1)$. In this outer part of the reaction centre it is found that

$$T \sim -\ln[\gamma\tau + \gamma B \psi^{1/n}] \sim p + O(1) \qquad 3.17$$

as $\tau \to 0$ with ψ/τ^n fixed, where B is a O(1) constant. When runaway takes place from a smooth initial maximum in T at $\psi = 0$ Jackson, et al, and Dold all find that $n = \tfrac{1}{2}$.

Temperature, pressure and reactant mass fraction all vary by O(1) amounts in brief, exponentially small, time-intervals after the establishment of runaway. Jackson, et al, describe this behaviour for locations close to the initial point of runaway, such as D in Fig.4, but it is more important for present purposes to turn to some very recent work by Dold and Kapila.

4. SINGULARITY PATHS AND COMBUSTION WAVES

The significant point is made in two recent works (Kapila and Dold, (1989) and Dold and Kapila, (1989)) that the runaway process, described in terms of a point-event at the end of the last Section, does in fact persist along a locus or path that may well be a continuous curve in ψ,t space which starts in a reaction centre RC. Such a locus has been called a singularity path since it is defined to be the set of points at which T and p, as solutions of (3.7-9), become logarithmically unbounded.

The appearance of such a locus in an asymptotic analysis is clear evidence that new physical behaviour is ocurring in its neighbourhood, specifically that the asymptotic forms (3.6) and (3.7-14) have broken down and that a new set of equations is necessary to describe the local behaviour.

Suppose for the present that a singularity path exists, say along $t = t_w(\psi)$. The proposition is that substantial changes in T, p, etc., occur with great rapidity as $t_w(\psi)$ is approached or crossed in, for example, the t-direction, whilst changes with t along $t_w(\psi)$, or lines parallel to the t_w-locus, are relatively very slow. Dold and Kapila define co-ordinates $\xi(= t_w - t)$ and ψ, and make $(\partial/\partial\psi)_\xi \ll (\partial/\partial\xi)_\psi$. Applied to the induction-domain equations (3.7-9) this leads to the conclusion that to leading order as $\xi \to 0+$ (i.e. from within I)

$$\tilde{T} \sim -\ln\{(\gamma - t_w'^2)\xi/(1-t_w'^2)\} \qquad 4.1$$

and

$$\tilde{T} \sim (\gamma - t_w'^2)\tilde{p} \; ; \; t_w' \cong dt_w/d\psi \; . \qquad 4.2$$

Comparing (4.1) with (3.17) shows that the singularity path near a point like D in Fig.4, where $t_w' \ll 1$, is given by

$$t_w \sim t_e + B\psi^{1/n} \; . \qquad 4.3$$

The quantity $1/t_w'$ is equal to the mass flux through the t_w-locus; (4.3) demonstrates that this mass flux is arbitrarily large as $\psi \to 0$ on t_w, so that t_w defines the location of an event that travels into $\psi > 0$ with very great (supersonic) speed, although this speed does diminish as one moves away from the "origin" (such as point D in Fig.4).

The structure of the "boundary layer" that develops round t_w is described to leading order, by application of the derivative orderings, described above, to the Euler equations (3.1-4). This amounts to replacing f_t by $-f_\xi$ and f_ψ by $t_w' f_\xi$ for any quantity f. As a consequence (3.1,2) show that

$$\{p + \gamma m^2 v\} - \{p_o(\psi) + \gamma m^2 v_o(\psi)\} \simeq 0 \; , \qquad 4.4$$

where m is the reciprocal of t_w'; (4.4) defines a Rayleigh line process. Exploiting (4.4) to write

$$vp_\xi = v_o p_\xi + (p - p_o)v_\xi$$

the energy equation (3.3) is re-written to read

$$2\gamma(pv)_\xi - (\gamma-1)\{(v+v_o)p_\xi + (p-p_o)v_\xi\} + 2\gamma Q c_\xi \simeq 0, \quad 4.5$$

which can be integrated to provide a Hugoniot relation (i.e. a p, v relation parameterised by c for any chosen ψ-value). Thus the "boundary-layers" around $t_w(\psi)$ have a quasi-steady structure that is determined by standard Rayleigh-line/Hugoiniot-curve analysis in addition, of course, to matching to the conditions determined by solutions of the I-domain equations, exemplified in (4.1,2).

The appearance of a singularity path in a solution of (3.14) indicates that a quasi-steady combustion wave, that carries substantial changes in all of the fluid properties, has been created in the field. Such a wave may propagate either supersonically (cf relation (4.3) and its consequences), in which case it is a weak detonation, or subsonically, in which case it is a fast flame.

Dold and Kapila (1989) have completed a thorough asymptotic analysis of the situation exhibited in Fig.4, and have described how the final ZND wave emerges as the weak detonation decellerates towards a CJ state. Figs.5 through 8 are broadly consistent with these findings.

The situation illustrated in Fig.2 differs from the one in Fig.4 by virtue of having a combustion wave included as part of the "initial" (i.e. $t=t_d$) conditions for the Euler problem. This means that the I region now includes a subsonic singularity path within its domains of dependence. Region I will therefore also be susceptible to influence from the hot "all-burnt" region to the left of the combustion wave; this quite complicated problem has yet to be considered in detail.

ACKNOWLEDGEMENTS

The author would like to thank Gurlat Singh for kindly providing him with the material for Figs.5 through 8. He is also most grateful to the University of Bristol for a Benjamin Meaker Visiting Professorship in the Department of Mathematics during 1988/89, which has provided opportunities for very profitable and enjoyable discussions with Dr. J.W. (Bill) Dold.

REFERENCES

BLYTHE, P.A. & CRIGHTON, D.G. (1989) Proc. R. Soc. Lond., A (in press)

CANT, R.S. (1984) Ph.D. Thesis, Cranfield Inst. of Tech.

CLARKE, J.F. (1981) Prog. in Aero. & Astro., 76, 383-402.

CLARKE, J.F. (1985) Chapter V in "The Mathematics of Combustion", ed. J.D. Buckmaster. SIAM, Pa.

CLARKE, J.F. & CANT, R.S. (1984). Prog. in Aero. & Astro., 95, 142-163.

CLARKE, J.F., Kassoy, D.R. & Riley, N. (1986) Proc. R. Soc. Lond., A 498, 129-148.

CLARKE, J.F. Kassoy, D.R., MEHARZI, N.E., RILEY, N. & VASANTHA, R. (1989) Proc. R. Soc. Lond., A, (submitted).

CLARKE, J.F. & SINGH, G. (1989) In "Numerical Combustion", eds. A. Dervieux and B. Larrouturou, Springer-Verlag, Heidelberg.

DOLD, J.W. (1988) Pages 461-470 in "Mathematical Modelling of Combustion", eds. C-M. Brauner and C. Schmidt-Laine, NATO ASI Series, Martinus Nijhoff, Dordrecht.

DOLD, J.W. & KAPILA, A.K. (1989) Proc. R. Soc. Lond., A, (submitted).

JACKSON, T.L., KAPILA, A.K. & STEWART, D.S. (1987) T. & A.M. Rept. No. 484, Univ. of Illinois.

KAPILA, A.K. & DOLD, J.W. (1989) Proc. 9th Symp. (Int.) on Detonation, 28 Aug.- 1 Sept. '89, Portland, Oregon (in press).

ORAN, E.S. & BORIS, J.P. (1981) Prog. Energy Comb. Sci., 7, 1-72.

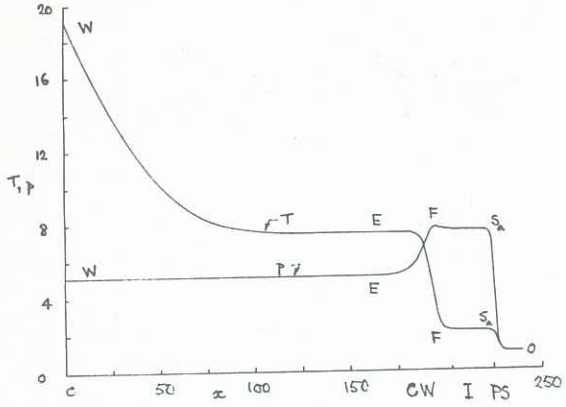

Fig.1 Temperature and pressure vs x at a fixed time t, $t_d < t < t_e$ (Fig.2) for flow driven by heat power

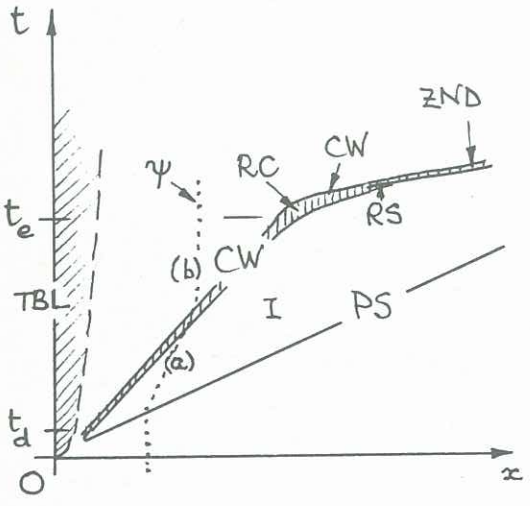

Fig.2 Distance-time diagram for flow driven by heat power (schematic).

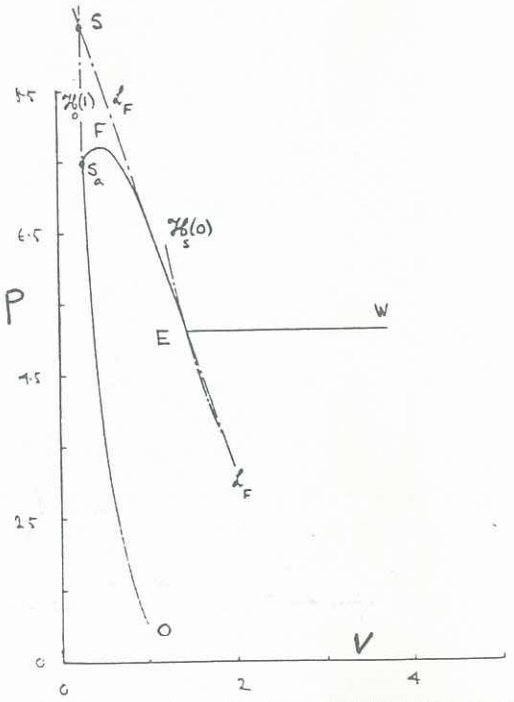

Fig.3 The p,v-plane for the profiles illustrated in Fig.1; note that lettering corresponds in the two figures.

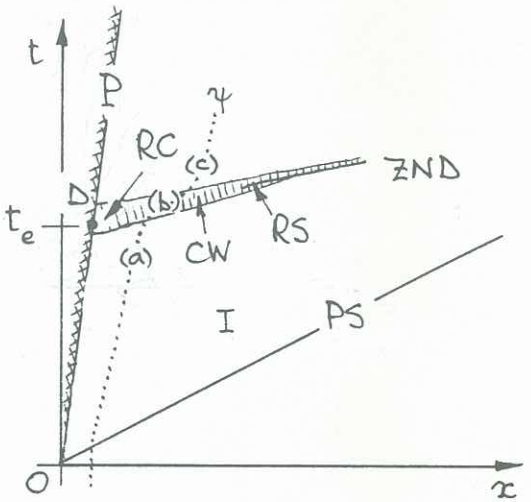

Fig.4 Distance-time diagram for flow driven by mechanical power (schematic).

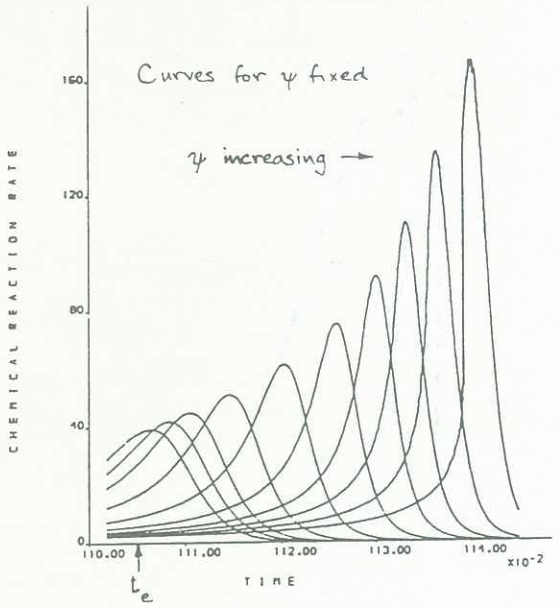

Fig. 5 Chemical reaction rate (cf (3.5)) vs. time for ten values of ψ (particle paths); mechanically driven field. $\psi = 6.2 \times 10^{-5}$, $(4.3 \& 8.4) \times 10^{-3}$, $(1.55, 2.5, 3.4, 4.17, 5.36, 6.14 \& 6.91) \times 10^{-2}$.

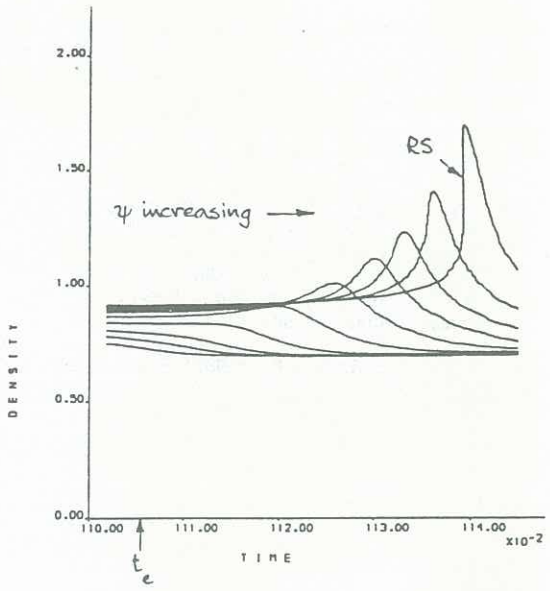

Fig.7 Density vs. time (cf caption for Fig.5)

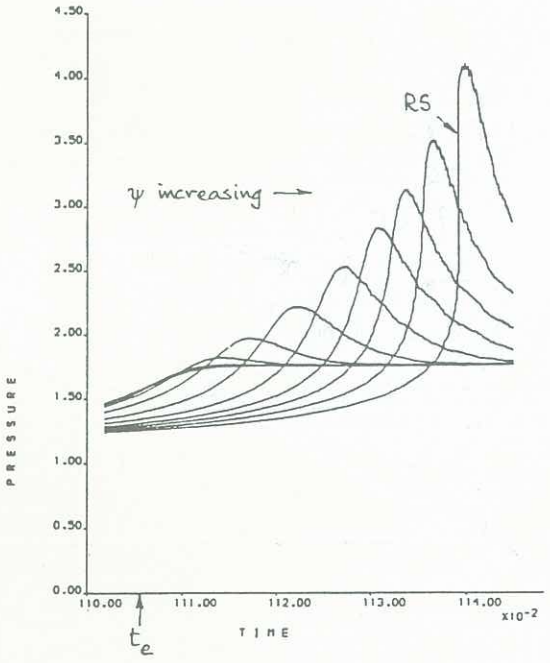

Fig. 6 Pressure vs. time (cf caption for Fig. 5)

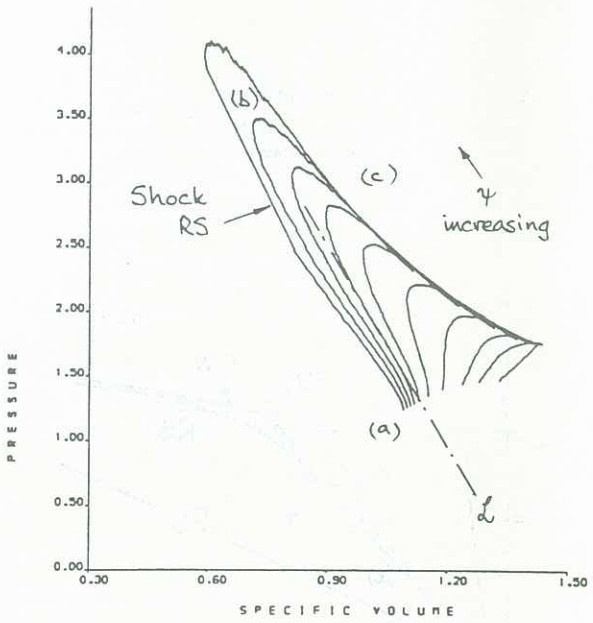

Fig.8 The p,v-plane (cf caption for Fig.5); regions (a), (b), (c) correspond with similarly labelled regions in Fig.4